Aerosol Science and Technology
Publication details, including instructions for authors and subscription information:
http://www.tandfonline.com/loi/uast20

Combined Optical and Ionization Measurement Techniques for Inexpensive Characterization of Micrometer and Submicrometer Aerosols

Charles D. Litton [a], Kirk R. Smith [b], Rufus Edwards [b c] & Tracy Allen [d]

[a] Pittsburgh Research Laboratory, NIOSH, CDC, Pittsburgh, Pennsylvania, USA

[b] School of Public Health, UC Berkeley, Berkeley, California, USA

[c] School of Social Ecology, UC Irvine, Irvine, California, USA

[d] EME Systems, Berkeley, California, USA

Available online: 06 Jan 2011

To cite this article: Charles D. Litton, Kirk R. Smith, Rufus Edwards & Tracy Allen (2004): Combined Optical and Ionization Measurement Techniques for Inexpensive Characterization of Micrometer and Submicrometer Aerosols, Aerosol Science and Technology, 38:11, 1054-1062

To link to this article: http://dx.doi.org/10.1080/027868290883333

Aerosol Science and Technology, 38:1054–1062, 2004

ISSN: 0278-6826 print / 1521-7388 online
DOI: 10.1080/027868290883333

Combined Optical and Ionization Measurement Techniques for Inexpensive Characterization of Micrometer and Submicrometer Aerosols

Charles D. Litton,[1] Kirk R. Smith,[2] Rufus Edwards,[2,3] and Tracy Allen[4]

[1] *Pittsburgh Research Laboratory, NIOSH, CDC, Pittsburgh, Pennsylvania, USA*
[2] *School of Public Health, UC Berkeley, Berkeley, California, USA*
[3] *School of Social Ecology, UC Irvine, Irvine, California, USA*
[4] *EME Systems, Berkeley, California, USA*

This article describes a simple combination ionization chamber and angular scattering sensor and presents the results of laboratory experiments to define its response to micrometer and submicrometer aerosols as a function of aerosol mass, surface, and diameter. The results of these experiments indicate that a simple theory is adequate to describe the operation of the sensor and presents correlations and techniques that will allow the sensor to be used for measurement and characterization of aerosols over a broad spectrum of possible applications related to adverse environmental and health consequences. For particles with volume mean diameters in the range of ~150–500 nm, the measured sensor responses yielded signal-to-noise ratios in the range of ~25 to > 500 for mass concentrations in the range of 0.50 to 16 mg/m^3.

INTRODUCTION

Measurement of micrometer (a few μm) and submicrometer (<1.0 μm) aerosol properties such as mass concentration, surface area, and diameter are important in understanding adverse health effects resulting from human exposure to aerosols. Currently available techniques and instrumentation necessary to conduct such measurements are generally complex, expensive, and often time-consuming to perform. Such instruments and techniques are used routinely in developed countries in mobile laboratories and ambient-air monitoring stations and are well-suited for measurements under controlled laboratory conditions. However, their routine use in real-world environments where better measurements of human exposure rather than ambient-air monitoring are needed in order to quantify adverse health effects is often difficult, if not impossible. To add to this difficulty, most applications require multiple measurements using several instruments over extended time periods. In some field measurements, locations may be remote and electrical power unavailable, so that use of these instruments is not possible. Of particular interest to us in this regard are monitors for use in developing countries to measure particle levels in and around households using solid fuels (biomass and coal). Such fuels are commonly used for cooking and heating, often resulting in high human exposure to particles and apparently contributing significantly to premature mortality and illness (Smith and Mehta 2003).

As particle concentrations are much higher in the developing world than average levels in developed countries, the risk attributable to particles from indoor and outdoor combustion of solid fuels is also much higher (Ezzati et al. 2002), and adverse health effects are seen in larger percentages of the population. Yet there is still much work to be done. Considering the large numbers of people in developing countries using different fuels at different periods of the year, and the increasing levels of particle pollution from modern-day risks such as transportation and industry, there is a clear need for economical monitoring devices that may be deployed in large numbers in the population in order to measure concentrations leading to both acute and long-term adverse effects. Current integrated assessment methods such as pumps, filters, and size-cut devices, however, are both relatively expensive, labor-intensive, require laboratory backup, and only reveal average multihour levels concentrations. Portable datalogging light-scattering devices are too expensive

Received 2 February 2004; accepted 25 August 2004.
Funding by the Household Energy and Health Programme of the Shell Foundation, UK, to develop a low-cost particle monitor for use in developing countries is gratefully acknowledged. Comments on an earlier draft by Michael Apte, Ashok Gadgil, and Edward (Ted) Zellers are much appreciated.
Address correspondence to Charles D. Litton, Pittsburgh Research Laboratory, NIOSH, CDC, P.O. Box 18070, Cochrans Mill Rd., Pittsburgh, PA 15236, USA. E-mail: chl3@cdc.gov

and often lack sufficient battery life for multiday use in remote field conditions.

Recent research (Litton 2002a, b), however, has indicated that simple, low-cost technology that has been available since the mid 1970s may provide a solution to many of these real-world measurement problems. For over 25 years, smoke detectors have been available for use in apartments, homes, offices, etc., as well as for use in industrial environments. These detectors operate on the principles of ion depletion (ionization-type detectors) or optical scattering (photoelectric-type detectors) by the smoke particles. Although it has been observed for years that the ionization-type detectors respond better to the smaller diameter particles produced from flaming combustion and the photoelectric-type detectors respond better to the larger diameter particles produced during smoldering combustion (Bukowski and Mulholland 1978), it was not until the late 1990s that detailed quantification of these responses was begun (Litton 2002a).

The differences in response between the two detectors were significant. Qualitatively, ionization-type detectors showed a higher response to smaller particles produced from the exhausts of diesel engines or flaming combustion, while photoelectric-type detectors showed little response. For the larger particles produced from smoldering combustion, just the reverse was true. In addition, it was found that both the ionization-type and the photoelectric-type detector responses correlated with the ratio of ionization to photoelectric signals, and further that these correlations were in opposite directions.

In an effort to explore the potential of this technique further and concurrently to fulfill the needs for low-cost particle monitors, a commercial smoke detector that combines ionization-chamber sensing and optical-scattering sensing was identified and modified so that real-time signals could be measured continuously. Three of these dual sensors were then exposed to aerosols with relatively narrow size distributions (σ_g in the range of 1.40–1.55) and with number mean diameters varying from about 100 nm to about 600 nm. The experiments, the results obtained, and the theory are discussed in the sections that follow. The results indicate that this simple device may be used for the determination of mass concentration, total particle surface area, specific surface area, and average particle diameter.

EXPERIMENTAL

Tests were conducted using a standard Underwriters Laboratories Inc. (UL) smoke box (Edwards and Morrow 1995) and a TSI, Inc. Model 3075/3076 Constant Output Atomizer (TSI, Inc. 2002), which used various solutions of dioctyl phthalate (DOP) in ethanol to produce aerosols of different geometric mean diameters and with geometric standard deviations in the range of 1.40–1.55. The sensors were placed on a platform within the smoke box and aerosols from the generator allowed to flow from the aerosol generator into the smoke box where two small internal fans were used to mix the incoming aerosols within the smoke box. The sensors were modified so that the voltage from the ionization chamber could be read directly. The optical portion of these sensors uses a light-emitting diode (LED) with an output wavelength of 880 nm and a photodiode that measures the intensity of scattered light at an angle of 45° from the forward direction. In the original detector, the LED was pulsed at intervals of 8 s, but to achieve more timely data and also in an effort to reduce background noise the circuitry was modified so that the LED could be pulsed every 1.25 s and a running average of the previous 8 pulses (10 s) recorded every 5 s. Similarly, the output from the ionization chamber was sampled 8 times every 10 s and the average of the previous 8 readings recorded every 5 s in order to coincide with the optical measurements.

The typical experimental procedure was to select a particular DOP in ethanol solution and allow the aerosol generator to stabilize its output for roughly 10 to 15 min prior to flowing the aerosol into the smoke box. The mass concentrations of aerosols within the smoke box were monitored using a tapered element oscillating microbalance (TEOM; Patashnick and Rupprecht 1986) that continuously sampled the aerosols from the smoke box at a constant flow of 3.0 l/min. Typically, it was necessary to flow the aerosols into the smoke box for a period of about 8 to 12 min before fairly stable mass concentrations and sensor signals were achieved. Since the sensors sample passively, movement of the aerosols into the sensors is primarily via diffusion and convection, assisted by the airflows resulting from the internal mixing fans. For some of the experiments, in addition to the TEOM data, a scanning mobility particle sizer (SMPS; TSI, Inc. Model 3936; TSI, Inc. 1999) was used to measure the size distribution of particles within the smoke box. As will be shown in the following sections, the detailed size distribution data obtained with the SMPS greatly enhanced understanding of the sensor responses.

A total of 85 experiments were conducted, corresponding to 12 different DOP/ethanol solutions. In 10 of these experiments (5 different DOP/ethanol solutions), precise particle size distribution data were acquired using the SMPS. In 11 of the experiments, the sensors were operated at applied voltages different than the standard applied voltage of 9.0 volts in order to assess the impact on sensitivity and noise at other voltages. Mass concentrations as measured by the TEOM varied from a low of 0.5 mg/m^3 to a high of 37.0 mg/m^3, with the overall average equal to 9.6 mg/m^3. In the analysis of the data, the TEOM mass concentrations were converted to gravimetric by dividing by a constant factor of 1.725 (Edwards et al. 2004). For all of the data, the ionization chamber sensitivities and angular scattering sensitivities were obtained by dividing the respective steady-state signals by the measured TEOM mass concentrations converted to gravimetric mass concentrations. For data from which particle size distributions were obtained, sensitivities per unit surface area, specific surface, and particle diameters were also obtained. It should also be noted that no corrections were made in the analysis for changes in temperature and humidity, which, however, did not vary significantly in these laboratory tests.

The Ionization Chamber

For the ionization chamber used in these sensors, ions are produced from alpha particles using a 0.8 μCi source of ^{241}Am with the face of the source covered by a thin layer of Pd, roughly 2 μm thick (E. Duran, private communication). The ionization chamber is constructed so that ions generated near the source are contained in a relatively small volume, resulting in a high volumetric ion generation rate. This portion of the ionization chamber is usually referred to as the *reference chamber*. Once the alpha particles exit this region, they enter a much larger volume, usually referred to as the *active chamber portion* of the ionization chamber, resulting in a much-reduced volumetric ion generation rate. In the plane that divides these two regions is a thin metal conductor, usually called the *collection electrode*, which is electrically isolated from the rest of the chamber. This electrode is connected directly to the input of a high-impedance integrated circuit that allows for the measurement of the electrostatic potential at the interface between reference and active chamber. Because of the differences in volumetric ion generation rates within these two regions, significant differences in ion concentrations occur, resulting in space charge effects that perturb the electric field and distort the potential, so that the potential on the floating collection electrode, called the *collection electrode voltage* (CEV), is significantly lower than what it would be if no ions were present. When aerosols enter the ionization chamber, they act as ion sinks and accelerate mutual neutralization of biopolar ion pairs, causing the CEV to increase. Figure 1 is a schematic of the ionization chamber used in the dual sensors.

The Optical Scattering Chamber

Figure 2 is a schematic of the optical scattering chamber used in the dual sensors. The light source is a pulsed light emitting diode (LED) with an output wavelength of 880 nm (E. Duran, private communication). The light scattered from aerosol particles entering this chamber is detected at a forward scattering angle of 45° by a photodiode from which the output is amplified and converted to volts.

THEORY

Background

The aerosol mass concentration sensitivity of an ionization chamber or an optical scattering device can be defined as the change in collection electrode voltage per unit aerosol mass concentration, ΔCEV/M (for the ionization chamber), or the change in optical scattering voltage per unit aerosol mass concentration, ΔV_θ/M (for the optical-scattering chamber). Both of these sensitivities are significantly dependent upon the size distribution of the aerosols. If these sensitivities could be defined when the sensor is exposed to some unknown aerosol, then the resultant mass concentration could be determined simply by dividing the voltage change (ΔCEV or ΔV_θ) by the corresponding sensitivity. However, for average particle diameters and size distributions of interest in the study of combustion-generated aerosols (diameters ranging from less than 100 nm to a few thousand nanometers), these sensitivities can vary by more than two orders of magnitude. For instance, for particles described by a lognormal distribution with a number mean diameter of 50 nm and a geometric standard deviation of 1.70, ΔCEV/M is about 1.78 V/(mg/m^3). For the same geometric standard deviation but with a number mean particle diameter of 1000 nm, ΔCEV/M is about 0.0044 V/(mg/m^3), or roughly 400 times smaller. The optical-scattering sensitivity, while increasing rather than decreasing with particle diameter, shows a similar sensitivity range. Thus, even though one could in principle use some average sensitivity value to calculate an aerosol mass concentration, this concentration may be over- or underestimated by significant factors due to a lack of knowledge about the particle size distribution.

In order to obtain more-accurate aerosol mass concentration sensitivities, and hence more-accurate mass concentrations, previous data obtained at our laboratory indicate that both the

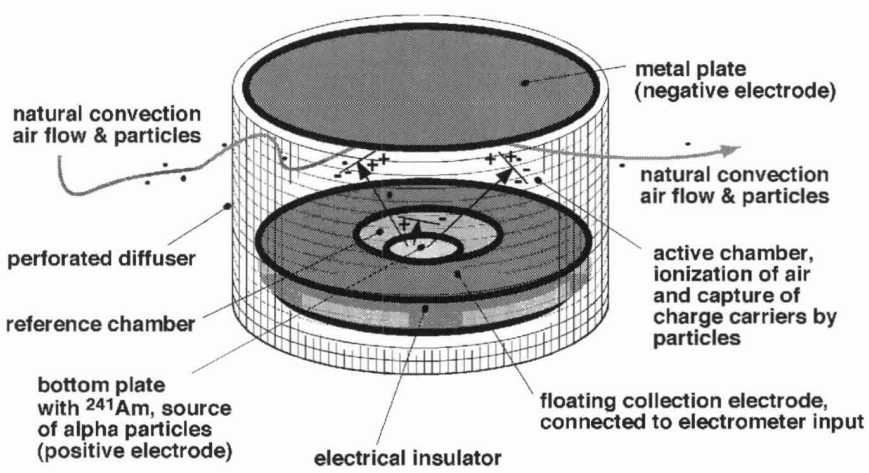

Figure 1. Schematic of the ionization chamber used in the dual sensors.

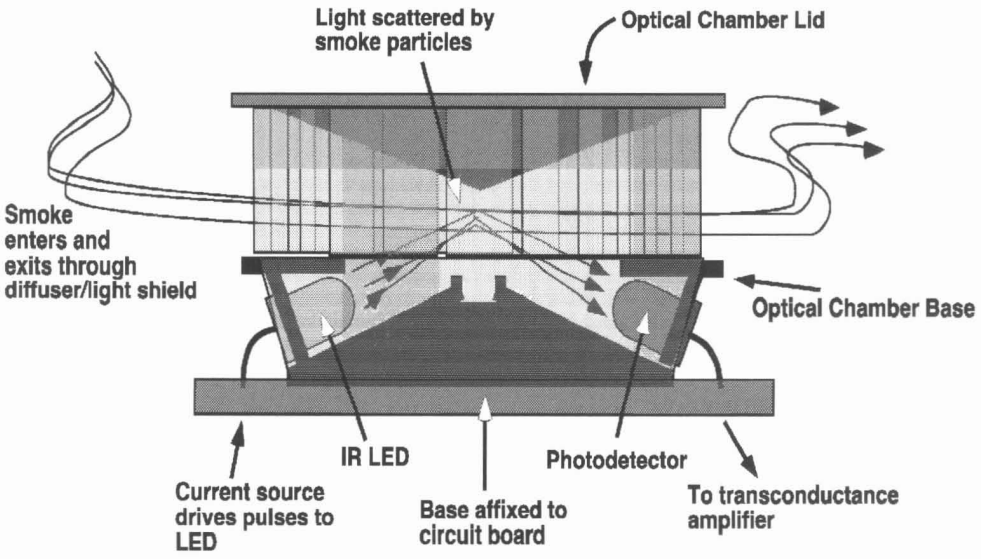

Figure 2. Schematic of the optical scattering chamber used in the dual sensors.

ionization-chamber sensitivity, ΔCEV/M, and the optical-scattering sensitivity, $\Delta V_\theta/M$, correlate with the dimensionless ratio, $\Delta CEV/\Delta V_\theta(3)$. For instance, at $\theta = 15°$, the correlations from Litton (2002a) for a broad range of combustion-generated aerosols, are shown in Figure 3.

The implications of such a correlation are that if both ΔCEV and ΔV_{15}, or the scattering at some other forward angle, are measured simultaneously, then the use of some empirical expression involving the ratio between them could allow for a much better definition of both the ionization-chamber sensitivity and the optical-scattering sensitivity. This, in turn, would allow a more accurate determination of the aerosol mass concentration. It is also worth noting that such correlations could be used in real time to automatically process the data provided that both optical and ionization-chamber signals satisfy adequate signal-to-noise constraints. In an effort to explore these correlations in greater detail and to define the theory for the observed correlations, the following section develops the theory for particles that can be described by a lognormal particle size distribution.

Theory for Lognormal Particle Size Distributions

In the following analysis, the moments of the lognormal particle size distribution weighted by number and defined by geometric number mean diameter, d_g, and geometric standard deviation, σ_g, lead to the following expressions for the count mean diameter, d_{10}, the diameter of average surface area, d_{20}, and the diameter of average mass, d_{30}:

$$d_{10} = d_g \exp\{1/2\,[\ln(\sigma_g)]^2\}, \quad [1]$$

$$d_{20} = d_g \exp\{[\ln(\sigma_g)]^2\}, \quad [2]$$

$$d_{30} = d_g \exp\{[1.5\ln(\sigma_g)]^2\}. \quad [3]$$

When N is the number of particles per cm^3, the diameters are in cm, the density, ρ, is assumed to be 1.0 g/cm^3, and spherical

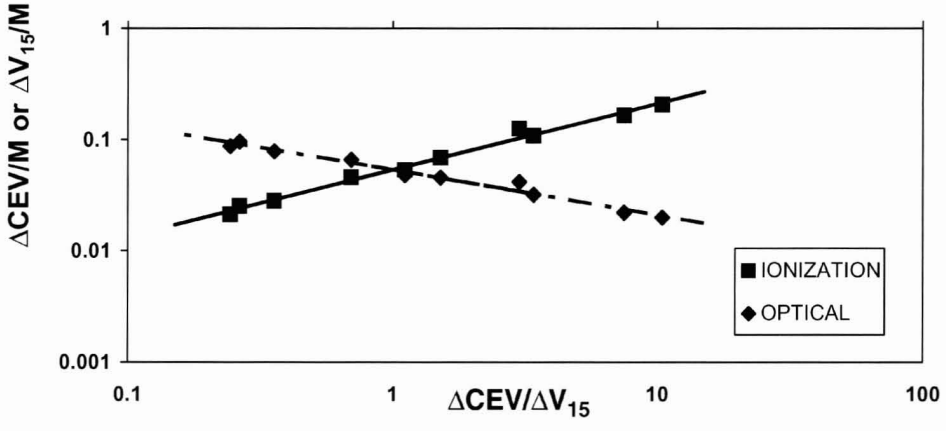

Figure 3. Correlation of ionization-chamber response per unit mass concentration (ΔCEV/M) and angular-scattering response per unit mass concentration ($\Delta V_{15}/M$) with the dimensionless ratio of ionization-chamber voltage to angular-scattering voltage measured at 15°, $\Delta CEV/\Delta V_{15}$. For these correlations, ΔCEV/M varied with the ratio, $\Delta CEV/\Delta V_{15}$, raised to the 0.60 power, while $\Delta V_{15}/M$ varied inversely with this ratio raised to the 0.40 power (Litton 2002a).

symmetry is assumed, the mass concentration, M, in mg/m^3, is given by

$$M = 1 \times 10^9(\pi/6)(d_{30})^3N. \quad [4]$$

In order to explicitly quantify the response of ionization chambers to aerosols, a mathematical model was used to predict the electric fields and potentials that result in the air space between two electrodes when ions are formed (Litton 1977). This leads to the following simple analytic expression that defines the ionization chamber response to aerosols:

$$\Delta CEV = (\Delta CEV)_{max}(1 - e^{-\alpha\beta N}), \quad [5]$$

where α is a constant that depends on the physical characteristics of the ionization chamber, β is the attachment coefficient of air-molecule ions to particles $= 2\pi D_i d_{10}$, D_i is the ion diffusion coefficient (cm^2/s), d_{10} is the count mean diameter (cm), N is the number concentration of particles (cm^{-3}), and $(\Delta CEV)_{max}$ is the maximum change in CEV (volts).

For small values of the exponential argument in Equation (5), a Taylor series expansion leads to the simpler Equation (6) below, where the product $\alpha(CEV)_{max}$ is set equal to 0.075.

If charge transfer occurs primarily via diffusion charging, then the change in collection electrode voltage, ΔCEV, is given by the approximate expression

$$\Delta CEV = (0.075)2\pi D_i d_{10} N. \quad [6]$$

Dividing Equation (6) by Equation (5) and substituting from Equations (2) and (4) yields the following expression for the ionization chamber sensitivity, in units of volts/(mg/m^3):

$$\Delta CEV/M = 9.0 \times 10^{-10} D_i\{\exp[-4[\ln(\sigma_g)]^2]\}/(d_g)^2. \quad [7]$$

Performing a similar analysis for optical scattering data leads to

$$\Delta V_\theta = A_\theta(\pi/4)(d_{10})^2 N\, I_\theta, \quad [8]$$

where the normalized angular scattering intensity, I_θ, is computed using the simple Barber and Hill Mie scattering algorithm (Barber and Hill 1990) for scattering from a sphere and integrated over the lognormal size distribution. It should be noted that I_θ is also a function of the diameter and will be discussed in a later portion of this section.

A_θ is a constant that depends upon the power of the light source, the responsivity of the photodiode, the gain of the electronics, and the geometry of the system.

For $\theta = 45°$, when Equation (8) is divided by Equation (5) and Equations (2) and (4) are substituted, the scattering sensitivity, $\Delta V_{45}/M$, is then given by the expression

$$\Delta V_{45}/M = [1.5 \times 10^{-9} A_{45}\{\exp[-3.5[\ln(\sigma_g)]^2]\}/d_g]I_{45}. \quad [9]$$

Since the total surface area of the particles per unit volume, S, is given by

$$S = \pi(d_{20})^2 N, \quad [10]$$

Equations (3), (6), and (10) can be combined to yield

$$\Delta CEV/S = 0.15\, D_i\{\exp[-1.5[\ln(\sigma_g)]^2]\}/d_g \quad [11]$$

and, Equations (3), (8), and (10) combined to yield

$$\Delta V_{45}/S = {}^1/_4\, A_{45}\{\exp[-[\ln(\sigma_g)]^2]\}I_{45}. \quad [12]$$

The ratio of either Equation (7) to Equation (9) or Equation (11) to Equation (12) leads to

$$\Delta CEV/\Delta V_{45} = (0.60\, D_i/A_{45})\{\exp[-{}^1/_2\,[\ln(\sigma_g)]^2]\}/(d_g\, I_{45}). \quad [13]$$

For particles with diameters greater than about 120 to 130 nm and less than the scattering wavelength (880 nm), the normalized angular intensities calculated from the Mie theory (I_{45}) vary with the cube of the particle diameter. This range of particle diameters corresponds to the range of diameters used in these experiments. For smaller particle diameters, I_{45} varies with the diameter raised to the fourth power (Rayleigh scattering), while for larger diameters, the variation with diameter decreases. Then, qualitatively, from Equation (13), the quantity $\Delta CEV/\Delta V_{45}$ should vary inversely with the fourth power of the diameter for particle sizes used in the current experiments. Since $\Delta CEV/M$ varies inversely with the square of the diameter, then $\Delta CEV/M$ should vary directly with the square root of the ratio, $\Delta CEV/\Delta V_{45}$. Similarly, $\Delta V_{45}/M$ should vary inversely with the square root of this ratio. For the surface sensitivity functions, $\Delta CEV/S$ should be expected to vary with the $^1/_4$ power of this ratio, while for $\Delta V_{45}/S$, the variation expected is inversely with the $^3/_4$ power. If the above expressions accurately describe the responses of the ionization chamber and the angular scattering, experimental data should result in correlations approximating the indicated dependencies on the ratio, $\Delta CEV/\Delta V_{45}$.

To calculate particle diameters and distributions from these measurements, the following approach was taken. Assuming Equation (7) to be a valid expression for the ionization chamber sensitivity, then for any measured value of $\Delta CEV/M$, this equation defines the allowable values of d_g and σ_g. In a similar manner, Equation (9) defines the angular-scattering intensity for the same system of particles. But, since the Mie intensity, I_{45}, cannot in general be expressed by a simple analytic function, this quantity must be calculated for every allowable value of d_g and σ_g. Consequently, then, for a given value of $\Delta CEV/M$ the corresponding allowable values of σ_g can then be determined for any value of d_g. An iterative procedure, using the simple Mie scattering algorithm, is then used to calculate I_{45} for all allowed values of d_g and σ_g until the value obtained yields the measured value of $\Delta V_{45}/M$. The results and implications of this analysis are discussed in the following section.

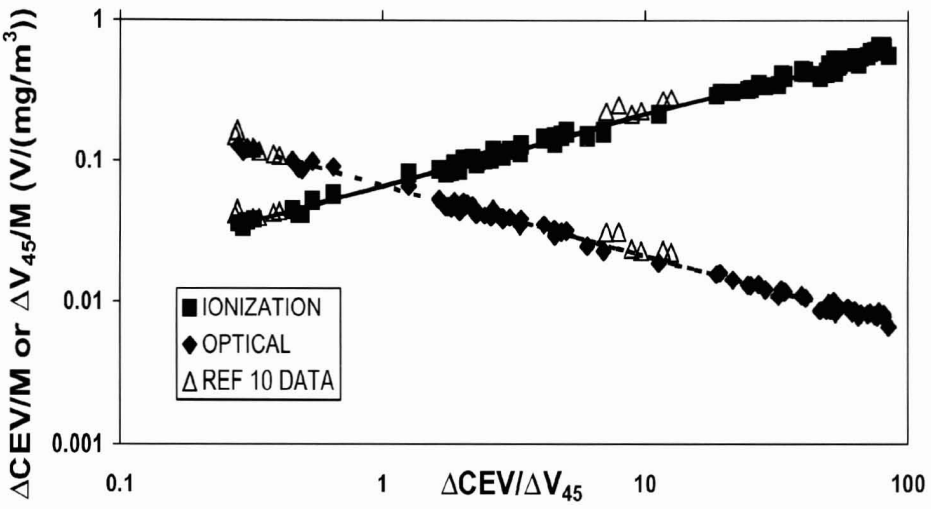

Figure 4. The sensitivities of the ionization chamber and optical scattering sensor, volts per unit gravimetric mass concentration V/(mg/m^3), as a function of the ratio, $\Delta CEV/\Delta V_{45}$.

RESULTS AND DISCUSSION

Correlations Involving Mass

Since the most common and acceptable measurement of aerosol concentrations is the mass concentration, the correlations of $\Delta CEV/M$ and $\Delta V_{45}/M$ are presented first in Figure 4 below, where the data are the average responses of all three sensors tested.

There were some differences in the responses of the individual sensors. For the ionization chamber sensors, these differences were slight, with the average overall difference only ±4.0% of the average response. However, for the optical sensors, one sensor consistently showed a greater sensitivity than the other two, with an average sensitivity 15.9% greater than the average of the other two. However, even including this consistent behavior, the average overall difference for the optical sensors was still quite acceptable at ±8.4% of the average response. Perhaps of even greater significance is the comparison of the expected theoretical response to the measured values. $\Delta CEV/M$ should vary with the square root of the ratio, $\Delta CEV/\Delta V_{45}$, while $\Delta V_{45}/M$ should vary inversely with the square root of this ratio. The solid curves in Figure 4 are the regression lines, and for the ionization chamber response, the regression analysis yielded an exponent of 0.5009 ($r^2 = 0.9965$) while for the optical response the regression analysis yielded an exponent of −0.5004 ($r^2 = 0.9963$), both values in excellent agreement with the predicted values of 0.50 and −0.50, respectively.

The data points appearing as the solid triangles in Figure 4 are for similar data reported in Edwards et al. (2004), where the sensor responses were measured using aerosols generated from solutions of oleic acid. For the ionization and optical responses, the resultant correlations are

$$\Delta CEV/M(V/(mg/m^3)) = 0.0665(\Delta CEV/\Delta V_{45})^{1/2}, \quad [14]$$

$$\Delta V_{45}/M(V/(mg/m^3)) = 0.0665(\Delta CEV/\Delta V_{45})^{-1/2}. \quad [15]$$

Ion Diffusion Coefficient and Optical Constant

Now, in order to extend the capabilities of this technique to aerosol surface area and diameter, mass concentrations and size distributions were obtained for five different DOP/ethanol solutions, with corresponding values of d_g in the range of 120–380 nm, and values of σ_g in the range of 1.38–1.56. For the ionization chambers, the measured responses and size distributions were used in Equation (7) to calculate the effective ion diffusion coefficient, D_i. For the optical responses, the Mie scattering intensities, I_{45}, were calculated for the measured particle size distributions, and then Equation (9) used to determine an empirical value for the constant, A_{45}.

The resulting average diffusion coefficient (D_i) was found to equal 0.1522 cm^2/s ± 0.00769. This value is 3 to 4 times the generally accepted value of 0.042 cm^2/s (14), and the reasons for this higher value are not clearly obvious. It may be that the movement of ions under the influence of an electric field provides some enhancement, or that the creation of ions via collisions with energetic alpha particles imparts additional momentum to the ions, also resulting in some enhancement. Regardless of the actual explanations, the fact that the measured variation in the empirical value is only ±5% is evidence that this value represents reality.

Using this value, then, Equation (7) can now be written as

$$\Delta CEV/M = 1.37 \times 10^{-10}\{\exp[-4[\ln(\sigma_g)]^2]\}/(d_g)^2. \quad [16]$$

Similarly, the optical constant, A_{45}, in Equation (9) was found to have a value of $8.667 \times 10^4 \pm 1.2 \times 10^4$. Although there is greater uncertainty in this value, it is felt that this is partly due to the higher sensitivity shown by one of the optical sensors, as discussed above. When this value is substituted into Equation (9), the result is

$$\Delta V_{45}/M = [1.3 \times 10^{-4}\{\exp[-3.5[\ln(\sigma_g)]^2]\}/d_g]\, I_{45}. \quad [17]$$

Equations (16) and (17) now quantify both the ionization and optical responses of the sensors per unit mass concentration.

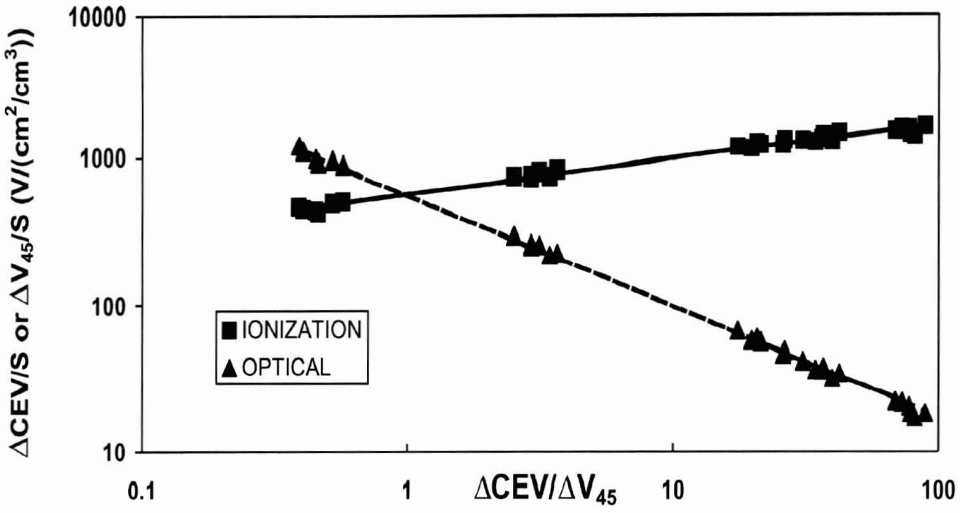

Figure 5. Correlation of ionization and optical responses per unit surface concentration with the ratio of ionization to optical response.

These expressions are also needed in order to compute particle diameters as discussed previously.

Correlations Involving Surface Area

From the particle size distribution data, Equations (4) and (5) may then be used to determine the number concentration of particles, N. Once these concentrations have been calculated, the total surface area per unit volume, S (cm^2/cm^3), can be determined from Equations (2) and (10), and the corresponding ionization and optical sensitivities per unit surface concentration calculated. Figure 5 shows the resultant correlations for the ionization and optical responses.

For the data of Figure 5, a regression analysis for the ionization response yielded an exponent of 0.236 ($r^2 = 0.9949$) compared to an expected value of 0.25, as discussed previously, while for the optical response, the regression analysis yielded an exponent of −0.765 ($r^2 = 0.9995$), compared to an expected value of −0.75. As for the mass correlations, there is excellent agreement between the experimental values and those expected theoretically. If it is assumed that the exponents expected theoretically are correct, then the following correlations result:

$$\Delta CEV/S\ (V/(cm^2/cm^3)) = 555(\Delta CEV/\Delta V_{45})^{1/4}, \quad [18]$$

$$\Delta V_{45}/S\ (V/(cm^2/cm^3)) = 555(\Delta CEV/\Delta V_{45})^{-3/4}. \quad [19]$$

In addition to these correlations, if Equation (14) is divided by Equation (18), or Equation (15) divided by Equation (19), an expression for the total particle surface area per unit mass can be obtained. The resulting expression is

$$S/M(cm^2/g) = 1.20 \times 10^5(\Delta CEV/\Delta V_{45})^{1/4}. \quad [20]$$

Determining Particle Diameters

Using Equations (16) and (17) and the method outlined in the previous section, estimates of particle diameter can be obtained. The results of this analysis are shown in Figure 6.

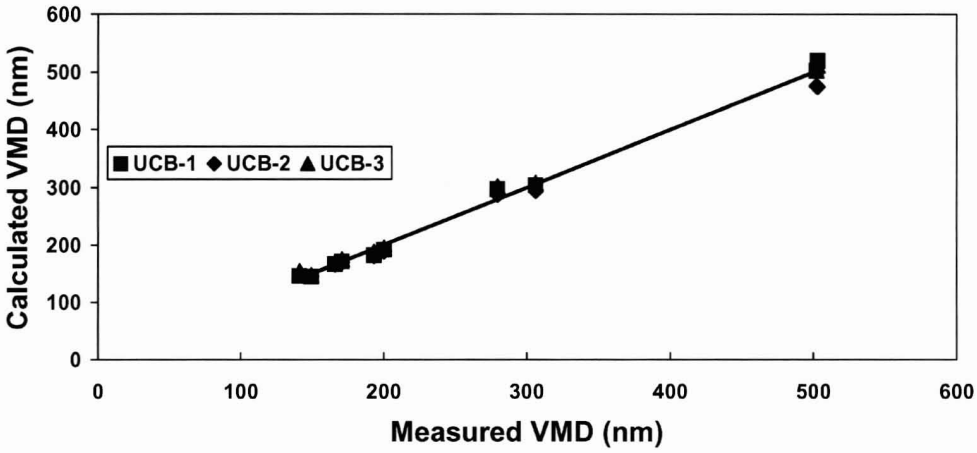

Figure 6. Calculated versus measured volume mean diameters (VMD) using the ionization/optical measurements.

In Figure 6, the volume mean diameters are presented rather than the values of d_g and σ_g, because the calculated values of d_g tended to be somewhat lower than the measured values (~12% lower) while the values of σ_g tended to be somewhat higher than the measured values (~10% higher). However, fortuitously the combination of lower values of d_g and higher values of σ_g resulted in calculated volume mean diameters in excellent agreement with those measured.

Application to Combustion Aerosols

Although these data were acquired using a system of relatively well-defined aerosols, extension to a wide variety of combustion-generated aerosols should be successful as well. Experiments to verify this expected behavior are underway, and the early indications are quite positive. For example, the response of the sensor to aerosols produced from flaming coal produced a dimensionless ratio, $\Delta CEV/\Delta V_{45}$, of 5.2. The above expressions would predict ionization and optical mass sensitivities of 0.152 and 0.029 V/(mg/m^3), respectively. The measured values were 0.14 and 0.031. Similarly, for aerosols produced from smoldering coal, the dimensionless ratio of 1.2 was obtained. Using this value, ionization and optical sensitivities of 0.073 and 0.061 could be predicted, compared to measured values of 0.075 and 0.058, respectively.

Operating the Sensor at Higher Applied Voltages

Tests were conducted at higher applied voltages than the standard 9.0 volts in order to determine the effect on sensitivity of the sensors. Since the sensors have an upper limit on the applied voltage of 15.0 volts, most of these data were acquired at an 12.0 volts. In addition to sensitivity measurements, additional tests were conducted to determine the average noise of the sensors both at 9.0 and 12.0 volts. Increasing the applied voltage from 9.0 to 12.0 volts resulted in an average increase in sensitivity per unit mass concentration for the ionization chamber of slightly greater than 30%, while the optical sensitivity was unchanged, as was expected. A further increase to 15.0 volts showed only a modest additional increase in sensitivity of about 3% for the ionization chamber.

Measurement Uncertainties

Although the data and analysis clearly indicate that these simple, inexpensive sensors have significant potential for continuous measurement of particle concentrations, the question naturally arises as to the potential uncertainty in these measurements due to signal fluctuations that are independent of the presence of particles, such as electronic noise or fluctuations due to changes in environmental conditions, such as temperature and relative humidity. Although it is beyond the scope of the present work to address in detail the impact of changes in temperature and relative humidity, model calculations for the ionization chamber response show slight to moderate decreases in CEV as a function of increasing temperature or relative humidity. Applying these theoretical corrections to particle-free experimental data has been quite successful, although additional experimental validation may be necessary for refinement of these corrections. For the optical component of the sensor, some slight variations in optical response have been observed due to temperature changes that may warrant further investigation.

To address the random electronic fluctuations in ionization chamber and optical scattering signals when no particles are present, the sensor signals were recorded over extended periods of time (typically, about 2 to 6 h), and the average signals and their standard deviation then computed. At an applied voltage of 9.0 volts, an average air temperature of 25.3°C, and an average relative humidity of 59.2%, the measured noise levels (noise defined to be one standard deviation from the average) for the ionization and optical signals were ±0.0129 and ±0.0015 volts, respectively. Increasing the applied voltage to 12.0 volts resulted in somewhat lower noise levels of ±0.0115 and ±0.0014 volts, respectively. Consequently, although little benefit was obtained for the optical component, the combined increase of 30% in sensitivity and somewhat lower noise levels indicates that operation at 12 volts could be beneficial for the ionization component. This aspect of the development warrants additional studies.

Due to the experimental procedure, it was not possible to obtain direct readings from the sensors as a function of mass concentration. However, for each steady-state mass concentration observed, there were corresponding steady-state outputs from the sensors. If the electronic noise levels discussed above are divided by the steady-state voltages observed for the sensors, and this ratio then multiplied by the corresponding steady-state mass concentrations, then it is possible to obtain an estimate of the noise equivalent mass concentrations, defined as the mass concentration at which the sensor signal-to-noise ratio is 1.0. This procedure was done for the range of particle diameters used in the experiments and the average noise equivalent mass concentrations for both the ionization and optical components then plotted versus the volume mean diameter. The result is shown in the following figure.

For these estimates, the ionization chamber has much lower noise equivalent mass concentrations for the smaller particles, corresponding to a greater sensitivity. For the larger particles, the optical-scattering chamber has much lower noise equivalent mass concentrations. Based upon these estimates and assuming that a signal-to-noise ratio (SNR) of 10 represents a reliable measurement, then for the particle size range shown in Figure 7, minimum mass concentrations in the range of 100 μg/m^3 to 700 μg/m^3 may be determined reliably.

For much smaller particles (VMD < ~140 nm), the increased sensitivity of the ionization chamber will allow for reliable determination of much lower mass concentrations. For instance, for particles with a VMD of 40 nm, mass concentrations of 20 μg/m^3 may be determined at a SNR ~10. For much larger particles (VMD > ~500 nm), the increased sensitivity of the optical scattering chamber will allow for reliable determination of much lower mass concentrations. For instance, for particles

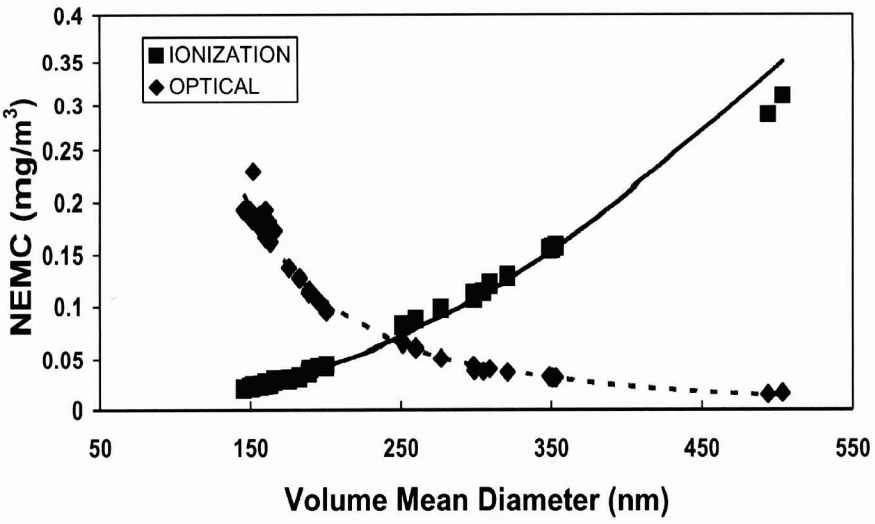

Figure 7. Noise equivalent mass concentrations (NEMC) for both the ionization chamber and the optical-scattering chamber plotted versus the volume mean diameters.

with a VMD of 1500 nm, mass concentrations of about 20 $\mu g/m^3$ may be determined at a SNR ~10. When exposed to higher mass concentrations (in the tens of mg/m^3) the sensor responses result in much higher SNRs and increased accuracy in the determination of mass concentrations. In addition, reductions in sensor noise levels will improve accuracy and result in the ability to determine even lower mass concentrations.

CONCLUSIONS

1. The data and analysis show that there is a direct relationship between both the ionization-chamber sensitivities and the angular-scattering sensitivities as a function of the dimensionless ratio of their signals. Measuring the voltage changes for both the ionization chamber and the optical-scattering chamber when exposed to some unknown aerosol and then forming the ratio of these voltage changes defines a unique sensitivity for both ionization and optical sensors that can subsequently be used to determine mass concentrations, surface concentrations, and specific surface area independent of any information about the particle size distribution. By using a simple iterative technique, reasonably accurate estimates of average particle diameters and size distributions may also be obtained.
2. The data and analysis also clearly show the high responsivity of ionization chambers for small particles (large ionization to optical response ratios) and the high responsivity of the optical-scattering sensors to larger particles (small ionization to optical response ratios). In actual data acquisition and analysis, these effects can be used to increase the reliability of the calculated mass or surface concentrations by using ionization chamber sensitivities when the ratio is high and the optical-scattering sensitivity when the ratio is low.
3. Increasing the applied voltage across the ionization chamber to 12 volts compared to 9 volts would increase sensitivity of the ionization chamber by about 30%.

REFERENCES

Barber, P. W., and Hill, S. C. (1990). In *Light Scattering by Particles: Computational Methods*, Singapore, World Scientific Publishing Co. Pte. Ltd., pp. 187–254.

Bukowski, R. W., and Mulholland, G. W. (1978). Smoke Detector Design and Smoke Properties, *NBS Technical Note 973*, Dept. of Commerce, National Bureau of Standards, Washington, DC.

Edwards, J. C., and Morrow, G. S (1995). Development of Coal Combustion Sensitivity Tests for Smoke Detectors, *U. S. Bureau of Mines Report of Investigations, 9551*. U.S. Government Printing Office, Washington, DC.

Edwards, R. D., Kirby, B., Smith, K. R., Hering, S., Allen, T., and Litton, C. D. (submitted). An Inexpensive Particle Monitor for Monitoring Combustion Smoke Concentrations in the Developing World: Laboratory Characterization, *JAWMA*.

Ezzati, M., Lopez, A. D., Rodgers, A., Vander Hoorn, S., Murray, C. J. L., and the Cooperative Risk Assessment Collaborating Group. (2002). Selected Major Risk Factors and Global and Regional Burden of Disease, *Lancet* 360:1347–1360.

Keefe, D., and Nolan, P. J. (1959). Charge Equilibrium in Aerosols According to the Boltzmann Law. *Proc. Royal Irish Acad.* 60:27–45.

Litton, C. D. (1977). A Mathematical Model for Ionization-Type Smoke Detectors and the Reduced Source Approximation, *Fire Technol.* 13:266–281.

Litton, C. D. (2002a). The Use of Light Scattering and Ion Chamber Responses for the Detection of Fires in Diesel Contaminated Atmospheres, *Fire Safety J.* 37:409–425.

Litton, C. D (2002b). Studies of the Measurement of Respirable Coal Dusts and Diesel Particulate Matter, *Meas. Sci. Technol.* 13:365–374.

Patashnick, H., and Rupprecht, G. (1986). Microweighing Goes On-line in Real Time, *Res. Dev.* 28:74–78.

Smith, K. R., and Mehta, S. (2003). The Burden of Disease from Indoor Air Pollution in Developing Countries: Comparison of Estimates, *Int. J. Hygiene Environ. Health* 20:279–289.

TSI, Inc. (1999). *Instruction Manual for Model 3936 Scanning Mobility Particle Sizer*, St. Paul, MN.

TSI, Inc. (2002). *Instruction Manual for Model 3075/3076 Constant Output Atomizer,* St. Paul, MN.